

1 **Supporting information**

2

3 **Exogenous ethanol induces a metabolic switch that prolongs the**
4 **survival of *C. elegans* dauer larva and enhances its resistance to**
5 **desiccation**

6

7 Damla Kaptan, Sider Penkov, Xingyu Zhang, Vamshidhar R. Gade, Bharath Kumar
8 Raghuraman, Roberta Galli, Júlio L. Sampaio, Robert Haase, Edmund Koch, Andrej
9 Shevchenko, Vasily Zaburdaev and Teymuras V. Kurzchalia

10

11

12 **Inventory of the supporting information**

13

- 14 1. Experimental procedures
15 2. References to supporting information
16 3. Legends to supplementary figures
17 4. Supplementary figures

18

19 **1. Experimental procedures**

20

21

22 **Worm strains and cultivation**

23 Wild-type strain used was *C. elegans* variant Bristol, strain N2. The following single
24 mutant strains were used in this study: DA2579 *sodh-1(ok2799) V*, CB1370 *daf-*
25 *2(e1370) III*, CB1372 *daf-7(e1372) III*, TJ1052 *age-1(hx546) II*. All *C. elegans* strains
26 were obtained from the Caenorhabditis Genetics Center (CGC). *daf-2(e1370);aak-*
27 *2(gt33)* double mutant was generated as described previously (Penkov et al., 2018).
28 During this study, the following strains have been generated:

29 *daf-2;aak-2;mitoGFP*: Males of *daf-2(e1370); zcIs14 [myo-3::GFP(mit)]*,
30 (dubbed *daf-2;mitoGFP*) were crossed to hermaphrodites of *daf-2(e1370);aak-2(gt33)*.
31 Males from the progeny were crossed to the mother strain *daf-2(e1370);aak-2(gt33)*.
32 Eggs from the resulting hermaphrodites were grown at 25°C and developed into dauers.
33 The dauers were left to recover at 15°C and eGFP-positive worms were selected and
34 singled. The progeny of these worms was selected based on the fluorescent signal. The
35 presence of *aak-2(gt33)* was tested by PCR.

36 *sodh-1;mitoGFP*: Males of *zcIs14 [myo-3::GFP(mit)]* (dubbed *mitoGFP*) were
37 crossed to hermaphrodites of *sodh-1(ok2799)*. Resulting hermaphrodites produced
38 eggs that were singled and selected for *sodh-1(ok2799)* via PCR and *mitoGFP* via
39 fluorescent signal.

40 Worms were routinely cultured on Nematode Growth Medium (NGM) plates
41 seeded with *E. Coli* NA22 strain(Brenner, 1974). Worms were placed on the plates
42 either as mixed stage populations or as embryos obtained by hypochlorite treatment.
43 Dauers were obtained by 1% SDS treatment of mixed stage populations from

44 overcrowded plates. Worms were collected from the feeding NGM-agar plates, washed
45 three times with ddH₂O, and resuspended in 10 ml of 1% SDS (w/v) in ddH₂O in 15
46 ml polypropylene centrifuge tubes (Corning, NY, USA). After 30 minutes of
47 incubation within the SDS solution at 25°C with shaking, the worms were washed
48 another three times with ddH₂O and placed on agarose plates where the alive worms
49 (dauers) were separated from the dead worms (non-dauers) based on their motility. The
50 temperature-sensitive Daf-c mutants were grown at 15 °C to grow in the reproductive
51 mode and at 25 °C to arrest as dauer larvae.

52 Worms were cultured on Nematode Growth Medium (NGM) plates seeded
53 with *E. Coli* NA22 strain (Brenner, 1974). Worms were placed on the plates either as
54 mixed stage populations or as embryos obtained by hypochlorite treatment. Dauers
55 were obtained by 1% SDS treatment of mixed stage populations from overcrowded
56 plates. Worms were collected from the feeding NGM-agar plates, washed three times
57 with ddH₂O and resuspended in 10 ml of 1% SDS (w/v) in ddH₂O in 15 ml
58 polypropylene centrifuge tubes (Corning, NY, USA). After 30 minutes of incubation
59 within the SDS solution at 25°C with shaking, the worms were washed another three
60 times with ddH₂O and placed on agarose plates where the alive worms (dauers) were
61 separated from the dead worms (non-dauers) based on their motility. The temperature-
62 sensitive Daf-c mutants were grown at 15 °C to grow in the reproductive mode and at
63 25 °C to arrest as dauer larvae.

64

65 **Dauer survival assay**

66 All dauer survival assays were performed in liquid. The inherent dispersive behavior
67 of dauer larvae obstructed the scoring of survival rates on solid medium as also

68 described by other groups (Narbonne & Roy, 2006). Dauers were incubated in 10 ml
69 Complete-S medium cultures supplied with designated ethanol concentrations or
70 without ethanol. No bacteria were added. Of note, the Complete-S medium contains
71 phosphates, sulfates, and a mix of trace metals (Stiernagle, 2006). Wherever
72 mentioned, a mixture of the following amino acids and ammonium chloride was
73 provided: L-Alanine, L-Arginine, L-Aspartate, L-Cysteine, L-Glutamate, Glycine, L-
74 Histidine, L-Isoleucine, L-Leucine, L-Lysine, L-Methionine, L-Phenylalanine, L-
75 Proline, L-serine, L-Threonine, L-Tyrosine, L-Valine. All amino acids and the
76 ammonium chloride were in 0.25 μ M final concentration, except L-cysteine, which
77 was 0.125 μ M. Similarly, wherever mentioned, a mixture of the following vitamins
78 was provided in final concentration: 4-Aminobenzoic acid (0.15 μ g/ml), D-Biotin
79 (0.075 μ g/ml), Folic acid (0.15 μ g/ml), Niacinamide (0.15 μ g/ml), D-Pantothenic acid
80 (0.15 μ g/ml), Pyridoxal (0.075 μ g/ml), Pyridoxine (0.15 μ g/ml), Riboflavin (0.15
81 μ g/ml), Thiamine (0.15 μ g/ml), D/L-6,8-Thioctic acid (0.075 μ g/ml). Cultures were
82 maintained shaking at 25 °C. Every week, aliquots containing around 50 worms were
83 scored for survival. The medium was renewed every week, thus maintaining the
84 concentration of ethanol, amino acids, and vitamins relatively constant and eliminating
85 waste products. Cultures were aerated approximately every 3.5 days.

86

87 **Desiccation tolerance assay**

88 Dauer larvae were prepared and treated with ethanol as described above. Samples for
89 desiccation were prepared as described before (Erkut et al., 2011). Shortly, dauer larvae
90 were collected in ddH₂O and transferred onto 3.5 cm plastic Petri dishes. The dishes
91 were placed in a chamber with controlled relative humidity (RH) at 98% RH and

92 incubated for four days. The samples were then either kept at 98% RH or transferred
93 into another chamber at 60% RH for one additional day. Ultimately, the worms were
94 rehydrated with ddH₂O for at least 2 h, transferred to NGM agar plates seeded with *E.*
95 *coli* NA22 and kept at 15 °C overnight to recover, after which survival was scored.

96

97 **2-Dimensional difference gel electrophoresis (2D-DIGE)**

98 Fifty micrograms of each protein sample (as determined using RC/DC kit) in urea lysis
99 buffer were labeled with 250 pmol CyDye DIGE Fluor dyes (GE Healthcare,
100 Germany). After labeling, excess dyes were quenched with 10 nmol L-lysine and the
101 samples were reduced in rehydration buffer (7 M urea, 2 M thiourea, 4% CHAPS (w/v),
102 and 50 mM DTT). The samples were pooled and supplemented with ampholytes
103 (BioLytes pH 3–10, BioRad, Germany) in a total volume of 350 µl. This labeled protein
104 mixture was loaded into an immobilized pH gradient strip (linear pH of 3–10) via
105 passive rehydration for 24 h. Following rehydration, isoelectric focusing was
106 performed in a Protean IEF cell (BioRad, Germany) for 55–60 kVh in total. The strip
107 was then equilibrated in equilibration buffer (6 M urea, 2% SDS (w/v), 50 mM Tris,
108 20% glycerol (v/v), and 130 mM DTT) for 10 min before being placed on a 20 cm wide
109 12% SDS-polyacrylamide gel. Proteins in the strip, along with PageRuler Plus
110 prestained protein weight marker (Fermentas, USA), were separated by SDS-PAGE at
111 200 V for 5 h. Finally, the gel was scanned using a Typhoon 9500 Fluo and Phospho
112 Imager (GE Healthcare, Germany) at 100 µm/pixel resolution for Cy2 (488 nm
113 excitation, BP 520/40 emission filter), Cy3 (532 nm excitation, BP 580/30 emission
114 filter), and Cy5 (633 nm excitation, BP 670/30 emission filter) at empirically
115 determined photomultiplier tube voltages. After laser scanning, gels were stained with

116 Coomassie blue and the spots of interest were cut out. The proteins in these gel slices
117 were extracted and characterized with geLC-MS/MS (Vasilj, Gentzel, Ueberham,
118 Gebhardt, & Shevchenko, 2012).

119

120 **MS Western quantification of the metabolic enzymes**

121 All reagents were of the analytical grade. LC-MS grade solvents were purchased from
122 Fisher Scientific (Waltham, MA); formic acid (FA) from Merck (Darmstadt,
123 Germany), Complete Ultra Protease Inhibitors from Roche (Mannheim, Germany);
124 Trypsin Gold, mass spectrometry grade, from Promega (Madison). Other common
125 chemicals and buffers were from Sigma-Aldrich (Munich, Germany). Protein
126 quantification was performed using Pierce BCA protein assay kit from Thermo
127 Scientific (Rockford, USA). Ampoules of Pierce BSA standard and isotopically
128 labeled $^{13}\text{C}_6$ $^{15}\text{N}_4$ -L-arginine and $^{13}\text{C}_6$ -L-lysine were purchased from Thermo Scientific
129 (Rockford, USA) and Silantes (Munich, Germany) respectively. Worms were washed
130 twice with M9 buffer, counted, collected and snap-frozen in liquid nitrogen for later
131 analysis. The frozen worms were thawed on ice and crushed using a micro hand mixer
132 (Carl Roth, Germany). The crude extract was centrifuged for 15 min. at 13,000 rpm at
133 4°C to remove any tissue debris. The clear supernatant was transferred to a fresh
134 Protein Lo-Bind tube (Eppendorf, Hamburg, Germany). The total protein content of
135 the samples was estimated using BCA assay and 15 µg of total protein content was
136 loaded to a precast 4 to 20% gradient 1-mm thick polyacrylamide mini-gels from
137 Anamed Elektrophorese (Rodau, Germany). Separate gels were run for the BSA and
138 isotopically labeled chimeric protein standard. Undetectable proteins or proteins
139 without detectable unique peptides (e.g., GPD-1, GPD-3, HXK-1, SODH-2 SUCL-1,

140 and SDHD-1) were not included. From the aldehyde dehydrogenase family, only the
141 peptides from ALH-1, ALH-9 and ALH-12 were included for absolute quantification
142 as the contribution of other family members to the total pool of ALHs was very small
143 (Fig. S3). The gels were processed according to the protocol described in (Kumar et
144 al., 2018). Peptide matching was carried out using Mascot v.2.2.04 software (Matrix
145 Science, London, UK) against *Caenorhabditis elegans* (November 2016) proteome
146 downloaded from Uniprot. A precursor mass tolerance of 5 ppm and fragment mass
147 tolerance of 0.03 Da was applied, fixed modification: carbamidomethyl (C); variable
148 modifications: acetyl (protein N terminus), oxidation (M); labels: $^{13}\text{C}(6)$ (K) and
149 $^{13}\text{C}(6)^{15}\text{N}(4)$ (R); cleavage specificity: trypsin, with up to 2 missed cleavages
150 allowed. Peptides having the ions score above 15 were accepted (significance threshold
151 $p < 0.05$). The chromatographic alignment and feature detection were carried using
152 Progenesis LC-MS v.4.1 (Nonlinear Dynamics, UK). The absolute quantification was
153 performed using in-house software. The label-free quantification and subsequent
154 statistical analysis were performed using MaxQuant (v 1.6.0.16) (Cox & Mann, 2008)
155 and Perseus (v1.6.2.1) (Tyanova et al., 2016), respectively.

156

157 **^{14}C -Ethanol Labeling**

158 Ethanol labeling was performed by directly incubating wild-type, *sodh-1(ok2977)*, and
159 *age-1(hx546)* dauers with 10 μCi of [^{14}C -EtOH] (Biotrend, Germany), in 10 ml
160 complete S-medium. After the incubation was completed, worms were washed three
161 times with ddH₂O and homogenized by five rounds of freezing in liquid nitrogen and
162 thawing in an ultrasound water bath. Organic compounds were extracted from
163 homogenized samples according to a standard method (Bligh & Dyer, 1957). Aqueous

164 fractions were dissolved in 50% CH₃OH, while organic fractions were dissolved in
165 CHCl₃:CH₃OH (1:2, v/v). Total radioactivity in each sample was measured using a
166 scintillation counter. Samples were normalized according to the number of worms, and
167 loaded on glass HPTLC plates (Merck, Darmstadt, Germany) covered with silicate.
168 2D-TLC of aqueous fractions for the visualization of hydrophilic metabolites was done
169 using 1-propanol–methanol–ammonia (32%)–water (28:8:7:7, v/v/v/v) as 1st system
170 and 1-butanol–acetone–glacial acetic acid–water (35:35:7:23, v/v/v/v) as the 2nd.
171 Lipids in organic fractions were analyzed by one-dimensional thin layer
172 chromatography (1D-TLC) with the solvent system chloroform-methanol-water
173 (45:18:3, v/v/v). TLC plates containing radioactive samples were sprayed with
174 EN³HANCE spray surface autoradiography enhancer (Perkin Elmer, Waltham, MA,
175 USA) and exposed to X-ray film (Kodak Biomax MR, Sigma-Aldrich, Taufkirchen,
176 Germany).

177

178 **HPLC-MS analysis of *C. elegans* metabolites**

179 About 20,000 dauer larvae were pelleted, washed three times, re-suspended in 500 µl
180 of LC-MS-grade H₂O (Merk, Darmstadt, Germany), and snap-frozen in liquid
181 nitrogen. The frozen pellet was freeze-sonicated 3-4 times until the lysate became
182 homogeneous. A volume of lysate corresponding to 50 µg total protein content was
183 diluted with LC-MS-grade H₂O to a total volume of 200 µl. 750 µl of chloroform-
184 methanol (1:2, v/v) were added and the mixture was shaken for 20 min. 250 µl of
185 CHCl₃ were added followed by vigorous shaking. Finally, 250 µl of LC-MS-grade H₂O
186 were added followed by vigorous shaking and centrifugation at 16,000 RCF for 5 min.
187 for phase separation. The upper phase (aqueous phase) was collected and dried under

188 nitrogen flow. The extract was re-suspended in 120 μ l of LC-MS-grade H₂O. For
189 HPLC-MS analysis, 20 μ l of the suspension were mixed to 80 μ l of 95% acetonitrile
190 and 20 μ l of this mixture were injected into a high performance liquid chromatography
191 (HPLC) system (1200 Agilent) coupled online to G2-S QToF (Waters). For
192 chromatographic separation a Bridge Amide 3.5 μ l (2.1x100mm) column (Waters) was
193 used. The mobile phase was composed of 95% acetonitrile, 0.5 mM CH₃COONH₄,
194 0,056 % NH₄OH (eluent A), and 40% acetonitrile, 0.5 mM CH₃COONH₄, 0,056 %
195 NH₄OH (eluent B). The following gradient program was used: Eluent B: from 0% to
196 100% for 15 min; 100% from 15min to 18min; 0% from 18 min to 25 min. The flow
197 rate was set at 0.5 ml/min. The spray voltage was set at 2.5 kV and the source
198 temperature at 150°C. Nitrogen was used as both cone gas (50 L/h) and desolvation gas
199 (1000 L/h). The desolvation temperature was 500°C. Spectra was acquired in negative
200 ionization polarity. The peak areas of the different metabolites were extracted from the
201 chromatogram using MassLynx software (Waters).

202

203 **CARS microscopy**

204 The imaging of lipid droplets was performed by coherent anti-Stokes Raman scattering
205 (CARS) microscopy (Camp Jr & Cicerone, 2015; Jungst, Winterhalder, & Zumbusch,
206 2011). CARS was detected using a multiphoton scanning microscope coupled with two
207 near-infrared picosecond fiber lasers. The optical microscope was an upright Axio
208 Examiner Z.1 equipped with a laser scanning module LSM 7 (all from Carl Zeiss
209 Microscopy GmbH, Jena, Germany) and multiple detectors in the non-descanned
210 configuration. The laser source used to excite the CARS signal (Femto Fiber pro TNIR
211 from Toptica Photonics AG) is tunable in the range 850 - 1100 nm and has a pulse

212 length of 0.8 ps. The wavelength was set to 1005 nm (emitted power at the source:1.5
213 mW), to resonantly excite the symmetric stretching vibration of methylene groups at
214 2850 cm^{-1} . The CARS signal was collected in transmission mode and selected using a
215 BP filter (640 ± 7) nm. A water immersion objective W Plan-Apochromat 20 \times /1.0 (Carl
216 Zeiss Microscopy GmbH) was used. Due to the transmission of optical elements, the
217 laser power in the sample was 52 mW. An automatic tiling procedure enabled by the
218 microscope software ZEN was used for the acquisition of images larger than the field
219 of view of the microscope objective. Multiple optical planes were acquired in z-stacks
220 covering all worm tissues containing lipid droplets. The total area of the lipid droplets
221 detected by CARS was calculated for all optical planes using Fiji (Schindelin et al.,
222 2012).

223

224 **Imaging of mitochondria**

225 For the visualization of mitoGFP by confocal microscopy, worms were mounted on 2%
226 agarose pads on glass slides (Thermo scientific, Superfrost Plus) and anesthetized with
227 500 mM levamisole in complete-S medium. The liquid was aspirated and the pads were
228 covered with coverslips (with 0.17 ± 0.005 mm cover slips (Menzel-Glaeser). The
229 mitoGFP was visualized with a Zeiss LSM 880 scanning confocal microscope equipped
230 with a Zeiss i LCI Plan-Neofluar 63x 1.3 Imm Korr DIC objective. eGFP was excited
231 at 488 nm, and fluorescence was detected at the emission band of 490-540 nm.
232 Depending on the depth of the tissue occupied by eGFP-marked mitochondria, single
233 or several adjacent optical planes were acquired. The mean circularity of mitochondria
234 was determined using shape descriptor analysis in Fiji (Schindelin et al., 2012) over all
235 objects in one image (for single planes) or a maximum z projection (for multiple

236 planes). The circularity of a particle was defined as $4\pi \times [Area] / [Perimeter]^2$, with a
237 value of 1.0 indicating a perfect circle. The nuclei, which are also marked with eGFP,
238 were manually annotated and removed from the analysis in advance.

239 This analysis was implemented as a macro for the current version of Fiji 2.0.0-
240 rc-69/1.52p. The code of the macro is available under the following link:
241 <https://doi.org/10.5281/zenodo.3918953>.

242

243 **Mathematical modeling**

244 To model the metabolic pathway (see Fig. 5A) of dauer larvae, we used the standard
245 way of describing chemical reactions as a system of ordinary differential equations for
246 the concentrations of participating components (Murray, 1989). For most of the
247 reactions, we applied standard equations of chemical kinetics with forward and
248 backward rates:

$$249 \quad \frac{da}{dt} = -(k_1 + k_4)a + k_2l + j_{in} \quad (1)$$

$$250 \quad \frac{dl}{dt} = k_1a - k_2l \quad (2)$$

$$251 \quad \frac{dc}{dt} = k_3k_2l \quad (3)$$

$$252 \quad \frac{dm}{dt} = -k_{d1}\Theta(k_4a - j_{min})m - k_{d2}\Theta(c_h - c)m \quad (4)$$

$$253 \quad \Theta = \begin{cases} 1 & \text{if } x \geq 0 \\ 0 & \text{if } x \leq 0 \end{cases} \quad (5)$$

254 Here a and l represented the concentrations of the acetate and lipid respectively, where
255 k_1 and k_2 are the forward and backward reaction rates for acetate to lipid conversion
256 (see below). Toxic compound concentration was denoted by c and it is produced from
257 the lipolysis with the rate k_3 . The consumption of acetate was also unidirectional with

258 the rate k_4 (see below). If there was exogenous ethanol, its presence was included via
 259 a constant influx j_{in} of acetate. The wellbeing of mitochondria was represented by a
 260 number denoted by m , which took values from 1 (completely functional mitochondria)
 261 to 0 (mitochondria completely damaged). Mitochondria could be damaged with a rate
 262 k_{d1} if the carbohydrate production, $k_4 a$, fell below a threshold j_{min} , or with a rate k_{d2}
 263 when the toxic compound c accumulated above a certain threshold c_h . Θ in Eq.(4)
 264 denotes the Heaviside step function as defined in Eq.(5).

265 While most of the reaction rates for simplicity were taken as constants, there
 266 were some rates that depended on chemical variables. One example was the dependence
 267 of k_4 on m , where we assumed that energy production requires functioning
 268 mitochondria and thus used a simple linear relation:

$$269 \quad k_4 = \tilde{k}_4 m,$$

270 where \tilde{k}_4 was a constant. Another rate that depended on concentrations was k_1
 271 denoting the conversion rate from acetate to lipids. It reflected the fact that there was a
 272 certain maximum amount of lipid l_s that could be possibly stored in a single worm and
 273 thus:

$$274 \quad k_1 = \tilde{k}_1 \frac{l_s - l}{l_1 + (l_s - l)}$$

275 Here l_1 was a constant determining at which lipid concentrations the conversion started
 276 to slow down and \tilde{k}_1 was also a constant. Finally, we chose k_2 rate to be of the
 277 Michaelis-Menten type:

$$278 \quad k_2 = \tilde{k}_2 \frac{1}{l_2 + l}$$

279 where \tilde{k}_2 and l_2 were constants.

280 Overall the above system of equations contains six independent parameters and
 281 requires the knowledge of the initial conditions for all four participating components.
 282 While measuring most of the involved rates and concentrations is potentially possible,
 283 it certainly goes beyond the scope of this manuscript. Instead, we chose the following
 284 strategy: We assumed that the model could predict a certain lifespan of wild-type or
 285 *daf-2* dauer (for simplicity, we do not mathematically distinguish between wild-type
 286 and *daf-2* because they have similar lifespans). We wanted to check, if there existed a
 287 region in the parameter space of the model, where, by having all parameters fixed and
 288 only changing those that would correspond to a certain mutation or a presence or
 289 absence of ethanol, we could reproduce the changes in the lifespan with respect to the
 290 wild-type/*daf-2* as was seen in the experiments.

291 Parameters used:

$\tilde{k}_{1(daf2)}/\tilde{k}_4$	9.0	l_1/l_2	0.1
$\tilde{k}_{1(age1)}/\tilde{k}_4$	3.0	j_{min}/l_2k_4	0.05
$\tilde{k}_{2(daf2)}l_2/\tilde{k}_4$	0.6	c_h/l_2	0.1
$\tilde{k}_{2(aak2)}l_2/\tilde{k}_4$	6.0	$a(t = 0)/l_2$	0.2
\tilde{k}_3/\tilde{k}_4	0.01	$l(t = 0)/l_2$	6.0
l_s/l_2	8.0	$j_{in}/l_2\tilde{k}_4$	0/0.09

292
 293 To model the pathway in *daf-2;aak-2* and *age-1* mutants, we modified the rates of the
 294 reactions regulated by AAK-2 and AGE-1 as illustrated on Fig. 5A. In the case of *daf-*
 295 *2;aak-2*, the only part in the model that is modified by the *aak-2* mutation is an
 296 increased \tilde{k}_2 . Correspondingly, we chose \tilde{k}_2 to be ten times larger than for a wild-

297 type/*daf-2* dauer. Regarding *age-1* mutants, we exploited the possibility that they may
298 have a reduced acetate to lipid transformation rate, which reduces both lipid
299 accumulation and toxic production. We tested this assumption by choosing k_1 of *age-*
300 1 mutant to be one-third of that in the wild-type/*daf-2* dauer. To solve the system of
301 differential equations, we used standard numerical integration tools in MATLAB.

302 **2. References to supporting information**

303

304 Bligh, E. G., & Dyer, W. J. (1957). A rapid method of total lipid extraction and
305 purification. *Can J Biochem Physiol*, 37, 911-917.

306 Brenner, S. (1974). The genetics of *Caenorhabditis elegans*. *Genetics*, 77(1), 71-94.

307 Camp Jr, C. H., & Cicerone, M. T. (2015). Chemically sensitive bioimaging with
308 coherent Raman scattering. *Nature Photonics*, 9(5), 295-305.

309 Cox, J., & Mann, M. (2008). MaxQuant enables high peptide identification rates,
310 individualized p.p.b.-range mass accuracies and proteome-wide protein quantification.
311 *Nat Biotechnol*, 26(12), 1367-1372. doi:10.1038/nbt.1511

312 Erkut, C., Penkov, S., Khesbak, H., Vorkel, D., Verbavatz, J. M., Fahmy, K., &
313 Kurzchalia, T. V. (2011). Trehalose renders the dauer larva of *Caenorhabditis elegans*
314 resistant to extreme desiccation. *Current biology : CB*, 21(15), 1331-1336.
315 doi:10.1016/j.cub.2011.06.064

316 Jungst, C., Winterhalder, M. J., & Zumbusch, A. (2011). Fast and long term lipid
317 droplet tracking with CARS microscopy. *J Biophotonics*, 4(6), 435-441.
318 doi:10.1002/jbio.201000120

319 Kumar, M., Joseph, S. R., Augsburg, M., Bogdanova, A., Drechsel, D., Vastenhouw,
320 N. L., . . . Shevchenko, A. (2018). MS Western, a Method of Multiplexed Absolute
321 Protein Quantification is a Practical Alternative to Western Blotting. *Molecular &*
322 *cellular proteomics : MCP*, 17(2), 384-396. doi:10.1074/mcp.O117.067082

323 Murray, J. D. (1989). *Mathematical biology*, vol. 19 of *Biomathematics*: Springer,
324 Berlin, Germany.

325 Narbonne, P., & Roy, R. (2006). Inhibition of germline proliferation during *C. elegans*
326 dauer development requires PTEN, LKB1 and AMPK signalling. *Development*, *133*(4),
327 611-619. doi:10.1242/dev.02232

328 Penkov, S., Erkut, C., Oertel, J., Galli, R., Vorkel, D., Verbavatz, J.-M., . . . Kurzchalia,
329 T. V. (2018). An insulin, AMPK, and steroid hormone-mediated metabolic switch
330 regulates the transition between growth and diapause in *C. elegans*.
331 *bioRxiv*. doi:10.1101/323956

332 Schindelin, J., Arganda-Carreras, I., Frise, E., Kaynig, V., Longair, M., Pietzsch, T., . .
333 . Cardona, A. (2012). Fiji: an open-source platform for biological-image analysis.
334 *Nature methods*, *9*(7), 676-682. doi:10.1038/nmeth.2019

335 Stiernagle, T. (2006). Maintenance of *C. elegans*. *WormBook : the online review of C.*
336 *elegans biology*, 1-11. doi:10.1895/wormbook.1.101.1

337 Tyanova, S., Temu, T., Sinitcyn, P., Carlson, A., Hein, M. Y., Geiger, T., . . . Cox, J.
338 (2016). The Perseus computational platform for comprehensive analysis of
339 (prote)omics data. *Nature methods*, *13*(9), 731-740. doi:10.1038/nmeth.3901

340 Vasilij, A., Gentzel, M., Ueberham, E., Gebhardt, R., & Shevchenko, A. (2012). Tissue
341 proteomics by one-dimensional gel electrophoresis combined with label-free protein
342 quantification. *J Proteome Res*, *11*(7), 3680-3689. doi:10.1021/pr300147z

343

344 **Legends to supplementary figures**

345

346 **Figure S1. Translational activation during exit from dauer state and induction of**
347 **alcohol-metabolizing enzymes by ethanol.**

348 2D-DIGE of proteins derived from wild-type dauers treated or untreated with food on
349 solid medium. Worms exit from dauer state and this process is accompanied by a global
350 translational activation as evidenced by the increase in multiple proteins (in green) in
351 food-treated worms. Representative images of two experiments.

352

353 **Figure S2. Treatment with ethanol leads to the accumulation of trehalose and a**
354 **higher turnover of amino acids and nucleotides.**

355 HPLC-MS analysis of the levels of various metabolites in untreated and ethanol-treated
356 wild-type dauers over time. Two biological replicates per time point are displayed.

357

358 **Figure S3. ALH-1 is the major aldehyde dehydrogenase that is upregulated upon**
359 **ethanol treatment.**

360 Relative proteomic quantification of the normalized abundances of all detectable ALH
361 members in untreated and ethanol-treated dauer larvae. The peptide abundances were
362 summed and normalized according to the abundance of the spiked-in BSA standard.

363 Error bars, \pm SD of two biological and two technical replicates.

364

365

366

367 **Figure S4. Dauers of *daf-2* survive moderately longer than wild-type dauers with**
368 **or without ethanol.**

369 The plot combines the mean survival rates of wild-type, *daf-2*, *daf-2;aak-2*, and *age-1*
370 dauers treated or untreated with 1 mM ethanol that are displayed in **Fig. 3D** and **F**.

371

372 **Figure S5. Exogenous ethanol rescues the desiccation tolerance of *daf-2;aak-2*.**

373 Mean survival of *daf-2* and *daf-2;aak-2* dauers untreated or incubated with 1 or 85 mM
374 ethanol followed by desiccation at various relative humidities (RH). Error bars \pm SD of
375 two biological with two technical replicates. For *daf-2* at 98%RH, n = 291 (day 0), 678
376 (day 3, no ethanol), 694 (day 3, 1 mM ethanol), 882 (day 3, 85 mM ethanol). For *daf-*
377 *2(e1370)* at 60% RH, n = 388 (day 0), n = 833 (day 3, no ethanol), n = 804 (day 3, 1
378 mM ethanol), n = 686 (day 3, 85 mM ethanol). For *daf-2;aak-2* at 98%RH, n = 504
379 (day 0), n = 533 (day 3, no ethanol), n = 260 (day 3, 1 mM ethanol), n = 1343 (day 3,
380 85 mM ethanol). For *daf-2;aak-2* at 60%RH, n = 388 (day 0), n = 282 (day 3, no
381 ethanol), n = 331 (day 3, 1mM ethanol), n = 859 (day 3, 85mM ethanol).

382

383 **Figure S6. The addition of exogenous amino acids and vitamins does not enhance**
384 **the survival rate of dauers treated with ethanol.**

385 Survival rates of wild-type dauers treated with ethanol, amino acids, and vitamins.

386 Means \pm SD of two-three biological replicates.

387

388 **Figure S7. Mathematical modeling of survival rates in *daf-2;aak-2* and *age-1***
389 **mutants.** Co-plotted are several other trends: “Acetate” is the combined entity
390 representing the free acetic acid and the acetyl-CoA produced in the pathway. “Lipid”

391 represents the bulk complex lipids, mainly TAGs, derived from the fatty acid
392 component. “Toxic” comprises the putative fatty acid-derived toxic compound(s).
393 “Mito” is defined by the degree of activity of the mitochondria and serves as a proxy to
394 the survival rate.

395 **A.** Model-predicted survival rates of *daf-2; aak-2* dauers without ethanol.

396 **B.** Model-predicted survival rates of *daf-2; aak-2* dauers treated with ethanol.

397 **C.** Model-predicted survival rates of *age-1* dauers without ethanol.

398 **D.** Model-predicted survival rates of *age-1* dauers treated with ethanol.

399

400 **Figure S8. *age-1* mutant dauer larvae have diminished incorporation of ¹⁴C-**
401 **ethanol into lipids.** Scintillation counting of radioactivity in the lipid-containing
402 organic fraction and aqueous fraction (containing hydrophilic metabolites such as
403 amino acids, sugars, nucleotides, etc.) of extracts from ¹⁴C-ethanol labeled wild-type
404 and *age-1* dauer larvae. Data obtained from two experiments, a total of 4 biological
405 replicates, two technical replicates each. Error bars, +SD. ** p<0.01; ns - no significant
406 difference determined by Student's *t*-test.

Supplementary Figures

Figure S1

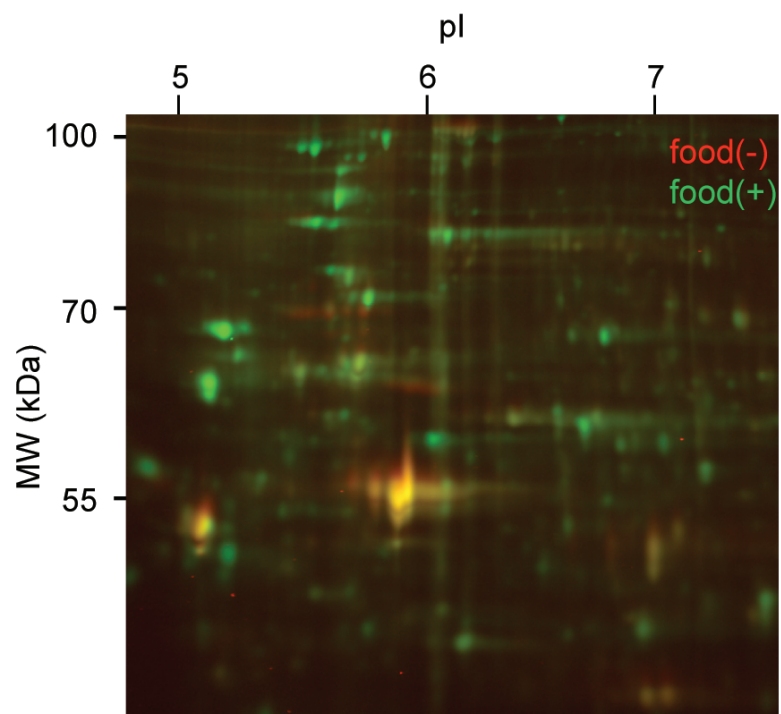


Figure S2

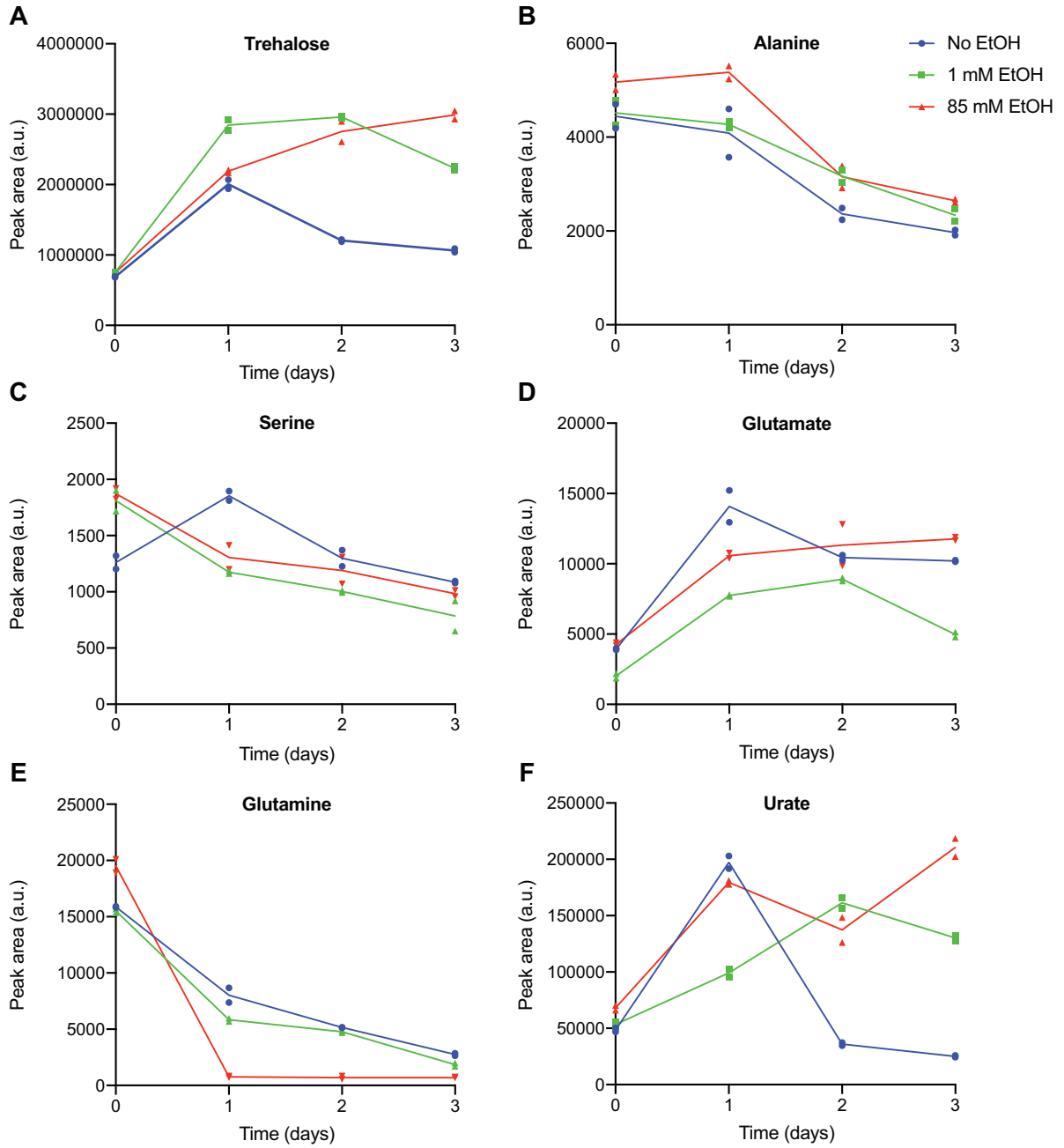


Figure S3

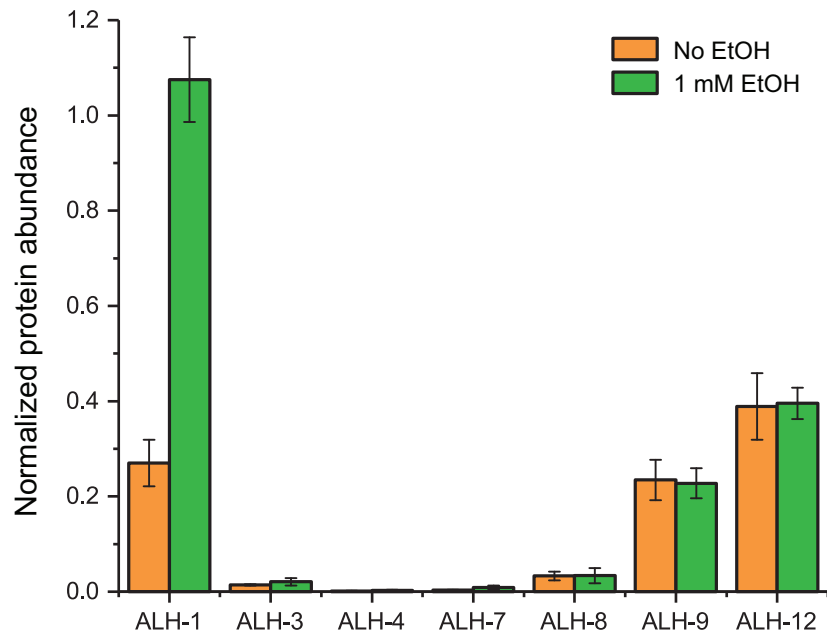


Figure S4

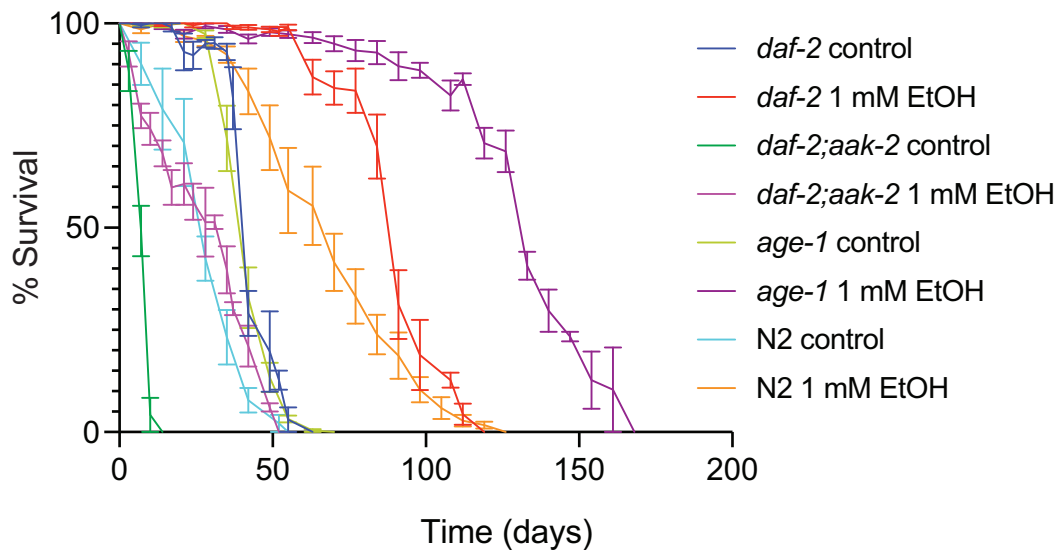


Figure S5

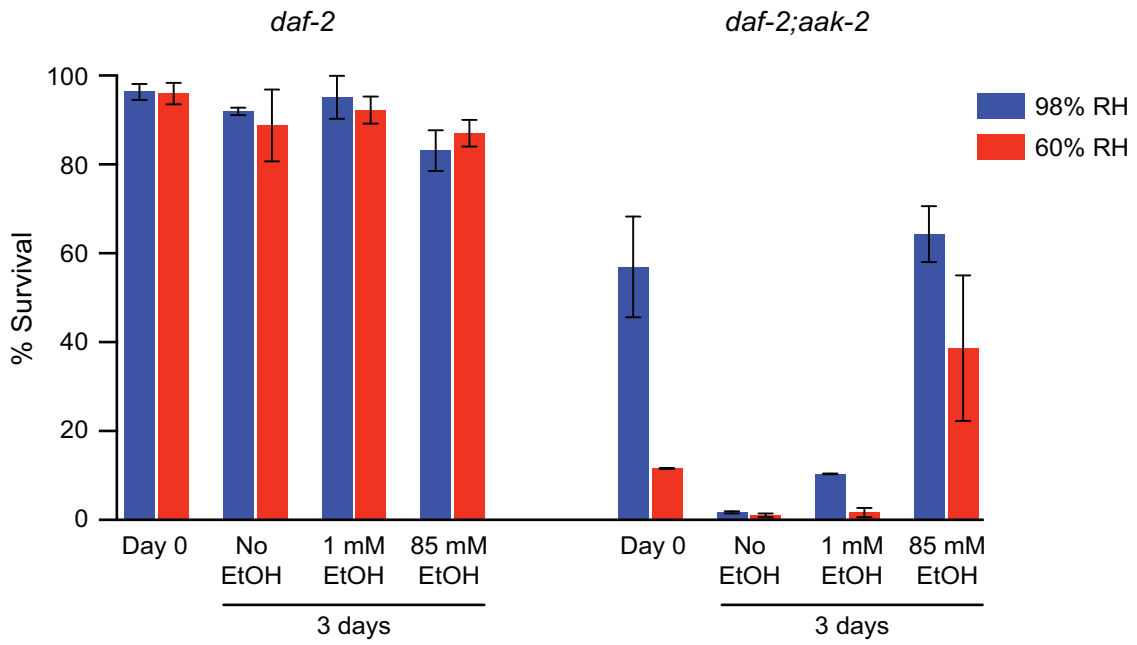


Figure S6

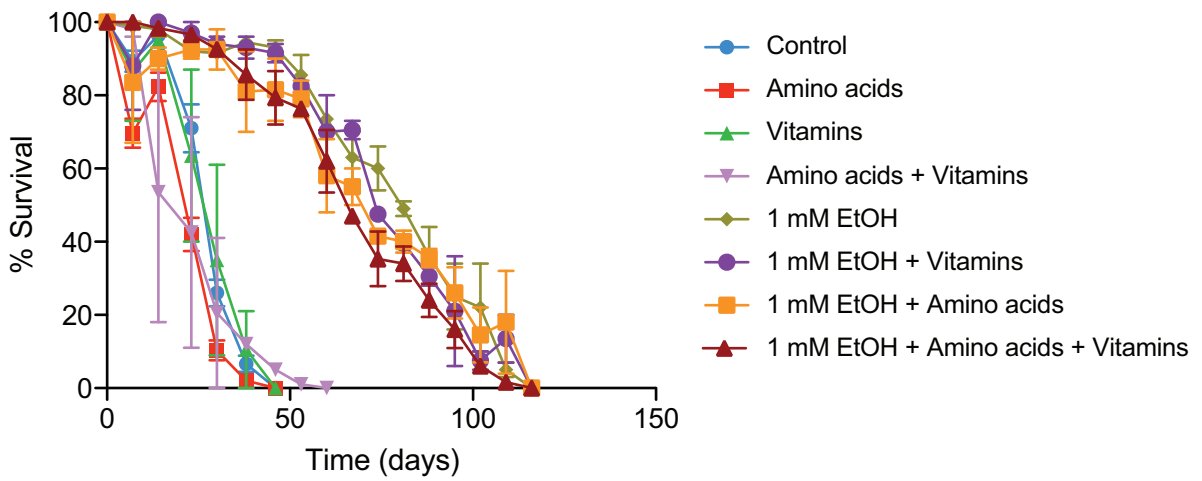


Figure S7

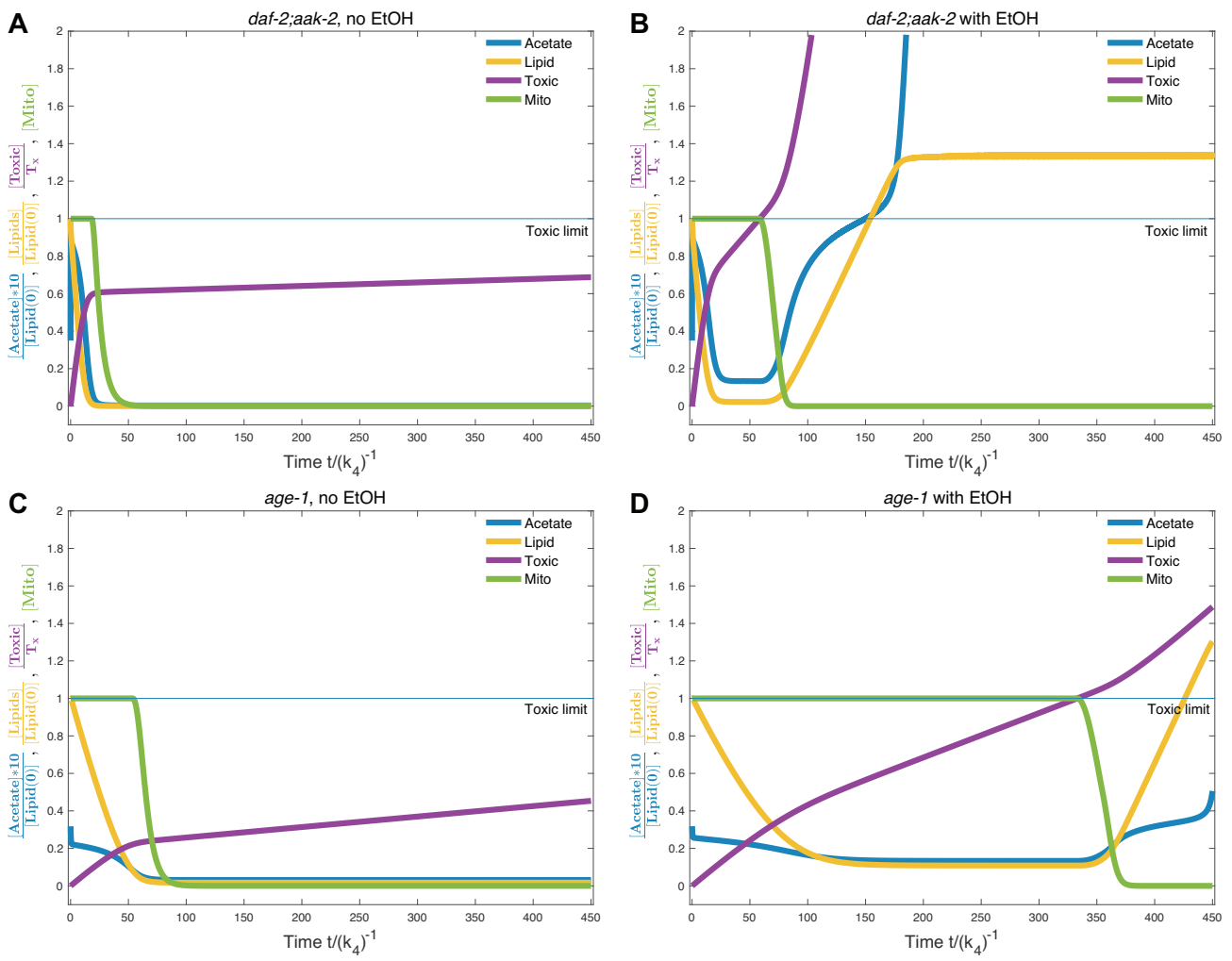


Figure S8

